Macromolecules

ARTICLE

pubs.acs.org/Macromolecules

Lamellar Bilayers as Reversible Sacrificial Bonds To Toughen Hydrogel: Hysteresis, Self-Recovery, Fatigue Resistance, and Crack Blunting

M. Anamul Haque,[†] Takayuki Kurokawa,[‡,§] Gen Kamita,[†] and J. Ping Gong*[,‡]

[†]Division of Biological Sciences, Graduate School of Science, Hokkaido University, Sapporo 060-0810, Japan

[‡]Faculty of Advanced Life Science, Hokkaido University, Sapporo 060-0810, Japan

[§]Creative Research Institution, Hokkaido University, Sapporo 001-0021, Japan

Supporting Information

ABSTRACT: We report the extraordinary toughness, hysteresis, self-recovery, and persistent fatigue resistance of an anisotropic hydrogel with single-domain lamellar structure, consisting of periodical stacking of several thousands of rigid, hydrophobic bilayers in the ductile, hydrophilic polymer matrix. The stratified lamellar bilayers not only diffract light to exhibit magnificent structural color but also serve as reversible sacrificial bonds that dissociate upon deformation, exhibiting large hysteresis as an energy dissipation mechanism. Both the molecular dissociation and lipid-like mobile nature of bilayers dramatically enhance the resistance to crack propagation by suppressing the stress concentration at the crack tip with the formation of extraordinary crack blunting. This unique toughening phenomenon could allow deep insight into the toughening mechanism of the hydrogel-like soft materials such as biological soft tissues.

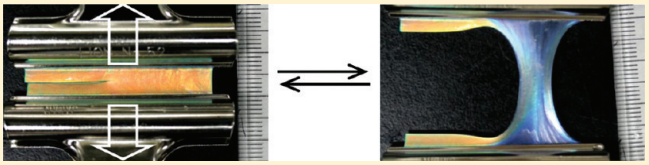

INTRODUCTION

The strength of a number of *hard and dry* materials, either natural, such as nacre[1−3] and shell,[4] or synthetic, such as ceramics,[5] is originated from their stratified structure consisting of alternatively stacked rigid and soft layers. For example, nacre is from brittle ceramic layers stacked in soft organic matrix.[3] Stratified structures also can be observed in *soft and wet* natural materials, such as muscle and blood vessel that exhibit high strength, toughness, and self-recovery of its function in response to successive mechanical stimulation.[6] These excellent mechanical performances are believed to be related to both the laminated and the soft and wet hydrogel-like structure, although the toughening mechanism remains poorly understood.[7,8] Creating soft and wet synthetic materials with excellent mechanical performances as that of load-bearing soft tissues had been a challenging task for material scientists. Most conventional soft and wet hydrogels usually show extremely poor mechanical performance due to their amorphous structure, in contrast with the natural biotissues that have well-defined hierarchy structure from molecular level to macroscopic scale. Although several hydrogels with high strength, such as slide ring (SR)[9] and tetra-PEG[10] gels, and toughness, such as nanocomposite (NC)[11] and double network (DN)[12,13] gels, have been successfully developed, they also possess amorphous structure. The SR and tetra-PEG gels showed an ideal elastic deformation, while NC and DN gels exhibited yielding and large hysteresis in tensile deformation as an energy dissipation mechanism.[13] To be a tough material, hysteresis is highly important because it is a measure of toughness of the materials.[13] The large hysteresis of the DN gel is related to the internal fracture of the brittle network, which avoids the stress concentration at the crack tip and dramatically enhances crack propagation resistance. That is, the brittle network serves as sacrificial bonds in the toughening of the DN gel. However, DN gel have negligible self-recovery and fatigue resistance due to the irreversible, permanent fracture of the chemical (covalent) bonds, which will be a limitation in many practical applications. So, if the brittle network is replaced by some reversible physical (noncovalent) bonds such as physical association, that damage upon loading and recovers back on unloading, these physical bonds serve as a reversible sacrificial bond to enhance toughness of chemically cross-linked gel exhibiting hysteresis and self-recovery. A wide variety of physical associations have been tried as reversible bond such as noncovalent interactions of poly(*N*,*N*-dimethylacrylamide) chain with silica nanoparticles[14] and ionic cross-linking in conjunction with a physically associated triblock copolymer network.[15] However, the former one has negligible dissipation in comparison with the tough DN gel, and the latter one has only the ability to recover about 50% of its initial dissipation.

One possible approach to remedy the above situation is the incorporation of self-assembled lipid-like bilayer structure into the polymer network in which the reversible noncovalent bond associated.[16] The hydrophobic association in conjugation with polymer bond might be served as a reversible (100%) sacrificial bond as it can polymerize itself. This system consists of hydrophobically associated bilayer structure of a polymerizable

Received: July 19, 2011
Revised: October 16, 2011
Published: October 31, 2011

Table 1. Swelling Degree, Water Content, Weight Fractions of PDGI and PAAm, and the Volume Fraction of the PDGI Bilayers of the Water-Swollen (Tested) Gel

[DGI][a] (mol L^{-1})	[AAm][b] (mol L^{-1})	swelling degree (w/w)	water content (wt %)	total polymer (wt %)	PDGI (wt %)	PAAm (wt %)	volume of PDGI bilayers (%)
0		49.0	97.90	2.10	0	2.10	
0.034		47.1	97.87	2.13	0.17	1.96	
0.067		38.5	97.40	2.60	0.39	2.21	
0.099	2.0	18.7	94.65	5.35	1.11	4.24	1.82
0.134		16.9	94.10	5.90	1.54	4.36	2.35
0.167		15.5	93.55	6.45	1.97	4.48	2.85
0.201		14.0	92.86	7.14	2.47	4.67	

[a] DGI concentration in the gel precursor solution. [b] AAm concentration in the gel precursor solution.

surfactant (dodecyl glyceryl itaconate:DGI) stacking inside polyacrylamide (PAAm) matrix. Initial development on this system is limited on the formation of bilayer structure only in the microscale which is randomly oriented in bulk hydrogel. It has been found that microscopically distributed bilayer structure contributes poorly to the bulk mechanical strength of the gel as stress concentrated easily in polymer network.[16] A macroscopic or centimeter scale and uniaxial bilayer structure in the bulk hydrogel might sustain large stress and dramatically enhance the bulk mechanical strength of the hydrogel. Recently, we have succeeded to synthesize the anisotropic hydrogel that has macroscopic unidomain lamellar structure, consisting of periodical stacking of several thousands of rigid, hydrophobic bilayers (PDGI) in the ductile, hydrophilic polymer (PAAm) matrix.[17]

In this work, we report the roles of uniaxial, stratified lamellar bilayers in the anisotropic hydrogel with an extraordinary toughness, hysteresis, self-recovery, and persistent fatigue resistance. The lamellar bilayers not only diffract light to exhibit magnificent structural color but also serve as reversible sacrificial bonds that dissociate upon deformation with huge energy dissipation. Both the molecular dissociation and lipid-like mobile nature of the bilayers dramatically enhance the resistance against crack propagation by forming an extraordinary blunting at the crack tip and give rise to the excellent mechanical performances of the hydrogel. The new toughening phenomena observed in this hydrogel might allow deep insight into the understanding of the toughening mechanism of biological soft tissues with laminated structure.

EXPERIMENTAL SECTION

Gel Preparation. PDGI/PAAm gel was prepared by simultaneous free radical polymerization from aqueous solution of 0−0.20 M dodecylglyceryl itaconate [DGI; n-$C_{12}H_{25}$−$OCOCH_2C(=CH_2)COOCH_2CH(OH)CH_2OH$], 0.025 mol % sodium dodecyl sulfate of DGI, 2 M acrylamide (AAm), 2 mM *N*,*N*′-methylenebis(acrylamide) as a cross-linker of AAm, and 2 mM Irgacure as an initiator. Plate-like gel sample with single-domain lamellar bilayer structure parallel to the substrate surface was achieved following the same procedure described in our previous paper.[17] Briefly, prior to the polymerization, by applying a shear flow to the precursor solution, thousands of lamellar bilayers of self-assembled DGI were aligned in one direction parallel to the surface of glass substrate. After polymerization, bilayers were stacked periodically and entrapped in the PAAm matrix to give a mechanically tough hydrogel after attaining equilibrium swelling in water. The degree of swelling of hydrogel was measured as the ratio of weight of the swollen hydrogel to weight of the dry hydrogel. The swelling degree, water contents (%), individual polymer (PDGI and PAAm) fractions (%), and the volume fraction of the PDGI bilayers (%) of the water swollen gel synthesized from various DGI concentrations were calculated, which are shown in Table 1. The volume fraction of the PDGI bilayers of the tested gel at low and high DGI concentration (<0.1 or >0.17 M) could not be calculated because of the absence of visible color in gel which provides the PAAm layer thickness.

Transmission Electron Microscopy (TEM). The hydrogel was cut into small pieces (2 mm × 2 mm × 1.2 mm) and then stained with osmium tetraoxide (OsO_4) for 5 days. After staining, the gel was immersed in water to attain equilibrium swelling state. The small pieces of gel were placed in a mold with specific shape, and a hardening resin was added to the mold in such a way that the samples keep its position in the middle of the resin. The gel samples that embed into the resin were dried in an oven for 48 h to obtain the dry gel sample embedded into the hard resin. Because of drying, the gel shrank to more than half of the initial thickness. The gel sample was fixed into the slice cutting machine (Ultracut; Leica EM UC6), and the resin was removed to make the cross section of gel to come out frontal. The cross section of the gel with a slice thickness of 200−500 nm was cut by a glass knife and placed on the grid to observe by a transmission electron microscope (Hitachi H-7650).

Small-Angle X-ray Scattering (SAXS). The swollen PDGI/PAAm gel with a thickness of ∼1 mm was cut into a small chip and then covered by two Kapton films. SAXS measurements were performed by exposing the X-ray beam from the side cross section of the plate-like gel sample, i.e., parallel to the bilayers direction at the BL40B2 of SPring-8, Japan Synchrotron Radiation Research Institute, using an incident X-ray with the wavelength, λ = 1.6 Å. Scattered X-rays were detected using an imaging plate with a resolution of 0.1 mm/pixel and a 3250 mm sample-to-detector distance.

Tensile Test. Tensile stress−strain properties of the gel samples were analyzed with a commercial test machine (Tensilon RTC-1310A, Orientec Co.). Prior to the test, the plate-like bulk gel was cut with dumbbell shape standardized size by the gel cutter (JIS-K6251-7) in such a way that the tensile elongation could be performed parallel to the top surface of the gel, i.e., in the direction along the lamellar bilayers.

Reflection Spectrum. The reflection spectrum measurements were carried out by using a Xe lamp for white light source. A photonic multichannel analyzer (Hamamatsu Photonics KK, C10027) was used for analyzing the detected signal. The entire reflection spectrum was obtained by keeping both the incident (Bragg's angle) and reflection angles at 60°, and the wavelength at maximum, λ_{max}, was obtained from the reflection spectrum. The reflection spectra of the gel at different tensile strains were measured by fixing the gel sample strongly at the jaws of slide caliper and the strain was achieved from the scale of slide caliper. The distance between two lamellar layers, d, was determined using the Bragg's law of diffraction, $2nd \sin\theta = \lambda$, where n = 1.33 (refractive index of water), θ is the Bragg angle or incident angle, and λ is the wavelength at maximum of the reflection spectrum.[17]

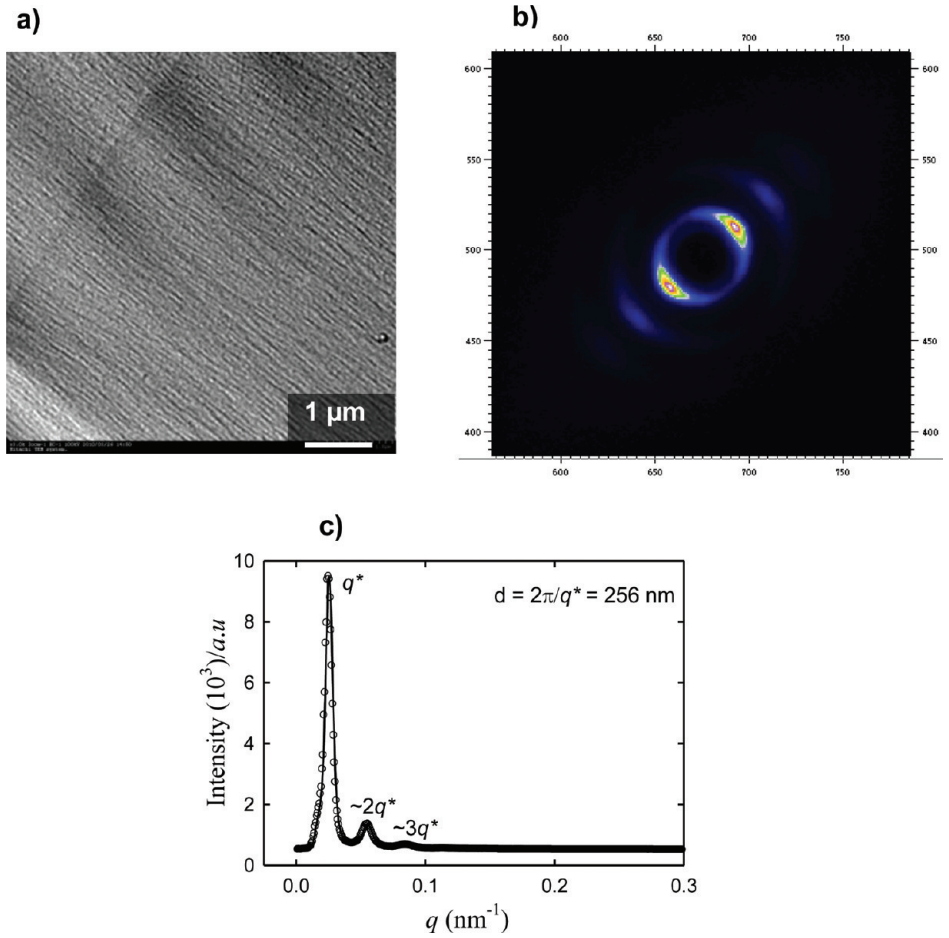

Figure 1. (a) Transmission electron microscope (TEM) image of the cross section of the gel show uniaxial orientation of bilayers and stratified structure of the PDGI/PAAm gel (0.10 M DGI). (b) Small-angle X-ray scattering (SAXS) image of the gel shows only perfectly anisotropic diffraction patterns demonstrating further the uniaxial orientation of bilayer structure. (c) Sharp first-order peak in the diffraction spectrum with the second- and third-order peak (an integer multiple of first-order peak) providing a *d* spacing of ~256 nm between two neighboring bilayers indicating the stratified pattern of bilayers inside the PAAm matrix.

Hysteresis and Cyclic Test. Hysteresis was observed by performing the tensile loading−unloading cycle in which the sample was initially stretched to a predefined strain and immediately unloaded at a fixed strain increasing/decreasing velocity. Similar loading−unloading cycles at increasing level of maximum strain were performed at various time intervals with the same sample. Multiple cycles at a fixed strain were performed by repeating the first cycles for the next four similar cycles at an interval of 0−30 min in between two successive cycles. All the loading−unloading cycles were performed by keeping the gel sample in water to prevent drying over the experimental time.

Pure Shear Fracture Test. For pure shear fracture test, an initial sharp notch/crack was created along the longitudinal direction of the gel which is in perpendicular to the bilayers. Two clips were fixed along the longitudinal direction of the gel keeping enough space on both side of the notch axis. The force was applied on the clips to elongate the gel perpendicular to the direction of initial notch/crack, and the photographs were taken at normal as well as different elongated states.

RESULTS AND DISCUSSION

Hierarchical Structure with Stratified Bilayers. The PDGI/PAAm hydrogel with uniaxial orientation of bilayers was synthesized by applying a shear flow to the precursor solution. The lamellar bilayer domains, which were randomly oriented in precursor solution, are successfully reoriented into the direction of the shear to form a single-domain lamellar structure.[17] After polymerization, the lamellar structure of the polymeric-DGI (PDGI) is immobilized inside the PAAm network, and we obtain an anisotropic hydrogel (water content: >90%) sheet with single-domain lamellar bilayers oriented parallel to the top surface of the gel. Although the polymerization reaction was carried out in one pot, both the DGI and AAm homopolymerized without reacting with each other while the two layers are linked through physical interaction and hydrogen bond.[18] The uniaxial bilayer structure of the PDGI/PAAm gel is confirmed from the very pure structural color of the gel and the transmission electron microscope (TEM) image (Figure 1a). The TEM image demonstrates the uniaxial orientation of bilayers parallel to the top surface of the gel. Small-angle X-ray scattering (Figure 1b,c) of water-swollen PDGI/PAAm gel demonstrates the true structural pattern of the gel. The clearly oriented diffraction pattern in SAXS image (Figure 1b) indicates the perfect anisotropic orientation of DGI molecules as well as their bilayers aggregates inside the PAAm matrix of the gel. The sharp first-order peak in the diffraction spectrum with the second- and third-order peak (an integer multiple of first-order peak) (Figure 1c) further justifies the anisotropic orientation and the stratified pattern of

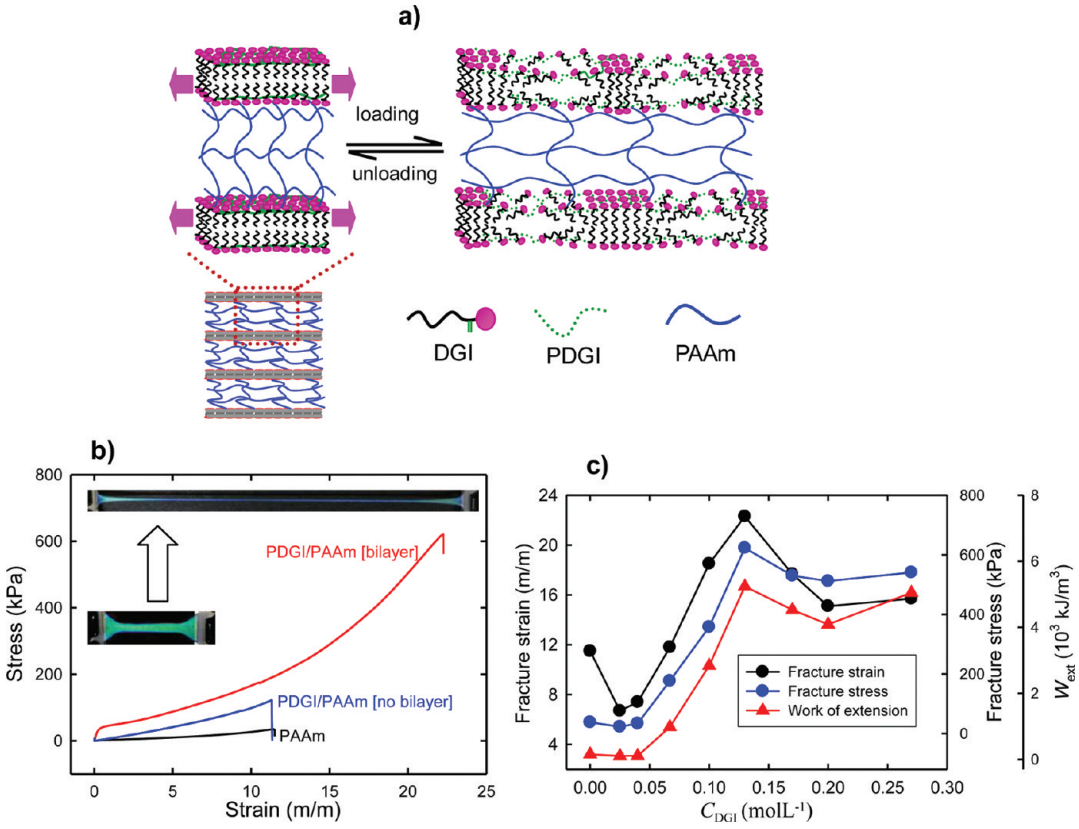

Figure 2. (a) An illustration of the stratified structure of PDGI/PAAm hydrogel consists of PDGI lamellar bilayers and PAAm matrix, and the fracture process of the bilayers on uniaxial elongation in the direction parallel to the bilayers. (b) Nominal stress as a function of strain at a stretching velocity of 200 mm/min for the PAAm gel and PDGI/PAAm gel with and without lamellar bilayer structure. The tensile deformation was performed along the lamellar bilayers direction as indicated by the illustration (a) and inserted images (b). The inserted images show the color change of the PDGI/PAAm gel from green to blue-violet upon elongation at a strain of 7. The concentration of DGI, AAm and MBAA at preparation were 0.13, 2.0, and 0.002 M, respectively. (c) Fracture strain (black ●), fracture stress (blue ●), and total work of extension at fracture (red ▲) as a function of DGI concentration indicates an optimum toughness.

bilayers inside the PAAm matrix. For the PDGI/PAAm gel with a specific composition (0.10 M DGI), the *d* spacing between two neighboring bilayers is calculated from SAXS spectrum as ~256 nm (Figure 1c), which is in agreement with the *d* spacing from Bragg's diffraction spectrum [λ_{max} = 596 nm (shown later) with corresponding *d* spacing as ~258 nm; calculated from Bragg's law[17]]. One can notice that the slight distortion of bilayer structure and the deviation of average interplane distance of the bilayers, *d*, in TEM images. This might be due to the shrinkage of the gel to more than half of the initial thickness during the drying of the gel sample (shrinking of soft PAAm networks) and distortion induced during the slicing of the cross section of the gel to obtain a slice with a thickness of 200−500 nm for the TEM observation. The inhomogeneous shrinking of PAAm might be occurred due to the common heterogeneity in chemical cross-linking of PAAm network.[19]

At room temperature, a single PDGI bilayer has a high modulus on the order of several MPa, and the PAAm matrix is much softer than the bilayer, with a modulus of few kPa depending on the cross-linker.[17] The thickness of one PDGI bilayer is 4.7 nm, and the distance between two next neighboring PDGI bilayers, *d*, is 150−300 nm depending on the DGI concentration and the swelling degree of PAAm networks.[17] Owing to the global uniaxial orientation of the lamellar bilayers, the gel has a strong anisotropy in its properties: it exhibits one-dimensional swelling in the direction perpendicular to the lamellar bilayers while the swelling in the direction of the bilayers is completely constrained.[17] The tensile modulus of the gel in the lamellar direction is ca. 10 times higher than the compressive modulus perpendicular to the lamellar bilayers.[17] Thus, the PDGI/PAAm hydrogel is said to have a stratified structure consisting of two alternating layer structures—one is rigid PDGI (not solid) and another is soft PAAm layers (Figure 2a)—similar to the structure found in some biological systems showing structural colors, such as in iridophore of tropical fishes[20] and nacre,[3,21] which is crucially important to be a tough material.

Tensile Strength and Yielding. By incorporating the uniaxial bilayers, the tensile strength of the PDGI/PAAm hydrogel is dramatically enhanced. During tensile elongation parallel to the bilayers direction, dissociation of bilayers into molecular states consumes a large amount of energy before complete fracture (Figure 2a). The tensile stress−strain curves for the PAAm gel, PDGI/PAAm gel having uniaxial bilayer structure, and the PDGI/PAAm gel without having uniaxial bilayer structure are shown in Figure 2b. The single PAAm gel fractured at a tensile stress and strain of 38 kPa and 11 m/m, respectively. Surprisingly, the fracture stress (~600 kPa) and strain (~22 m/m) of the PDGI/PAAm gel that has uniaxial bilayer structure are dramatically improved with exhibiting a clear yielding at low strain of the stress−strain curve. Accompanying with the tensile

dx.doi.org/10.1021/ma201653t |*Macromolecules* 2011, 44, 8916–8924

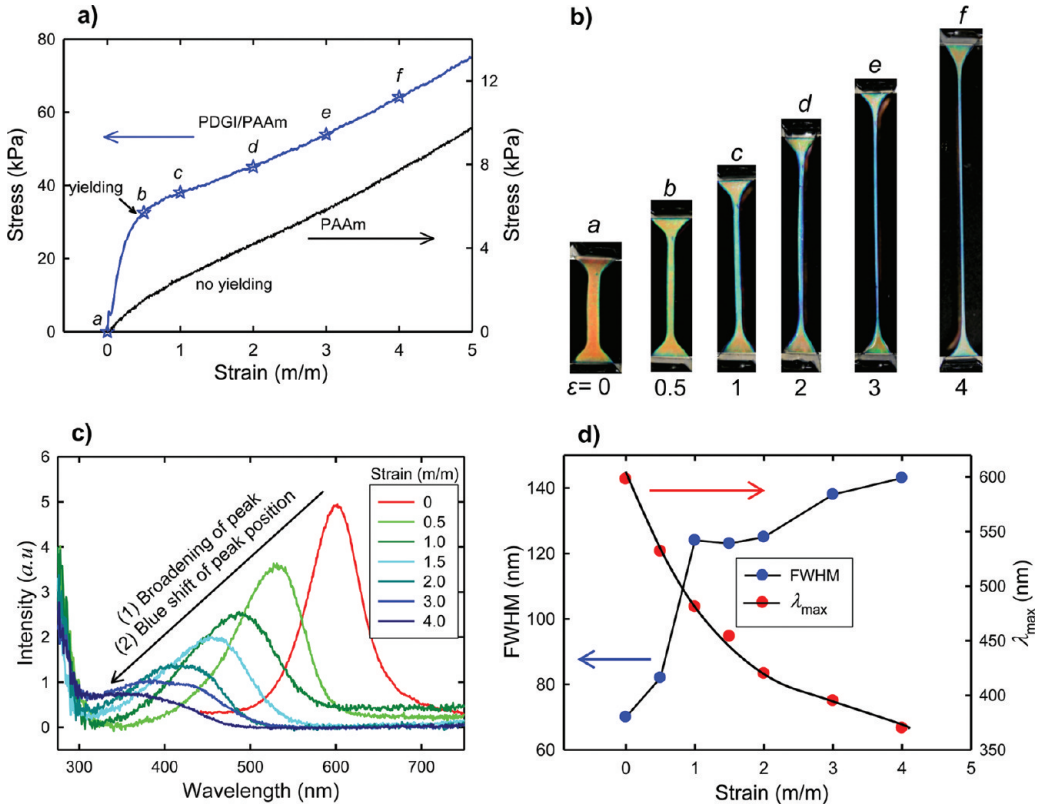

Figure 3. (a) Tensile stress−strain curve with clear yielding of PDGI/PAAm gel of 0.10 M DGI concentration and (b) the images of the gel taken at various tensile strain (ε). (c) The reflection spectra of the gel at different tensile strain show the peak broadening and blue shift of the gel color with gradual increase in strain. Both the Bragg's angle or incident angle and reflection angle were kept at 60° for the reflection spectrum measurement. (d) The wavelength at maximum (λ_{max}) and the full width at half-maximum (fwhm) of the reflection peak as a function of tensile strain. The yielding phenomenon of the gel is correlated to the bilayer structure collapse upon tensile deformation, as indicated by the abrupt increase of fwhm. No yielding occurs in the PAAm gel, as indicated by the inserted figure in (a).

deformation, the color of the gel changed from green to blue, which is shown by the inserted images of Figure 2b. In sharp contrast, the PDGI/PAAm gel that has no bilayer structure as well as color shows a stress−strain curve without yielding similar to that of the PAAm gel, only with a slight increase in the modulus and fracture stress.

We further observed the stress−strain behavior of the PDGI/PAAm gel prepared at different DGI concentrations (Figure S1). The PDGI/PAAm gels that contain low concentration of DGI also do not show yielding and fractured at low stress and strain due to the absence of bilayer aggregates of PDGI at that concentration, but the gel with a concentration of DGI, at which bilayer aggregates formed, shows sharp yielding with improved fracture stress and strain (Figure S1). The tensile properties of the gels prepared at different DGI concentrations are summarized in Figure 2c, which demonstrates the fracture strain, fracture stress, and total work of extension at fracture (W_{ext}) as a function of DGI concentrations. An optimum tensile strength of the PDGI/PAAm gel with an intermediate DGI concentration (0.13 M) is noticed. The large enhancement of the tensile strength of the gel is attributed to the unidomain bilayer structure inside the polymer network.

The yielding that observed at low strain of the stress−strain curve of PDGI/PAAm gel is shown in Figure 3a. Apparently, the yielding arises from the hydrophobically packed PDGI lamellar bilayers. The yielding reveals the structural change of bilayer packing beyond a certain strain, which might be caused either by the plastic deformation or by dissociation of hydrophobically aggregated PDGI bilayers (Figure 2a). As the gel exhibits color due to the Bragg's diffraction of visible light on the periodic lamellar bilayer planes, the structural change can be simply justified by the reflection spectrum of the gel under deformation. The photographs of the gel taken at different tensile strains (ε) are shown in Figure 3b. Elongation is accompanied by a compressive deformation perpendicular to the elongation direction, which results in a color change of the gel from reddish-orange to greenish-blue and then blue-violet (Movie-1). It is found that the corresponding reflection spectra taken at various elongation states show the shift in reflection peak to shorter wavelength and peak broadening continuously with the increase in strain (Figure 3c). The wavelength at maximum of the reflection peak (λ_{max}) and full width at half-maximum (fwhm) against the strain are shown in Figure 3d.

The λ_{max} decreased monotonously with increase in strain, but fwhm increased abruptly just above yielding strain ($\varepsilon_{yield} \sim 0.5$). This indicates a large disruption in periodical ordering as a result of yielding. Above this strain, the fwhm increased slowly, indicating small change in periodical ordering. On the other hand, single PAAm gel exhibits much smaller and pure elastic deformation without yielding (Figure 3a). The slight curvature appeared at low strain (~0.5) of PAAm gel is a feature of chemically cross-linked gel.[22]

Hysteresis and Self-Recovery. The feature of the sacrificial bonds in this material, hysteresis, is visualized by the systematic

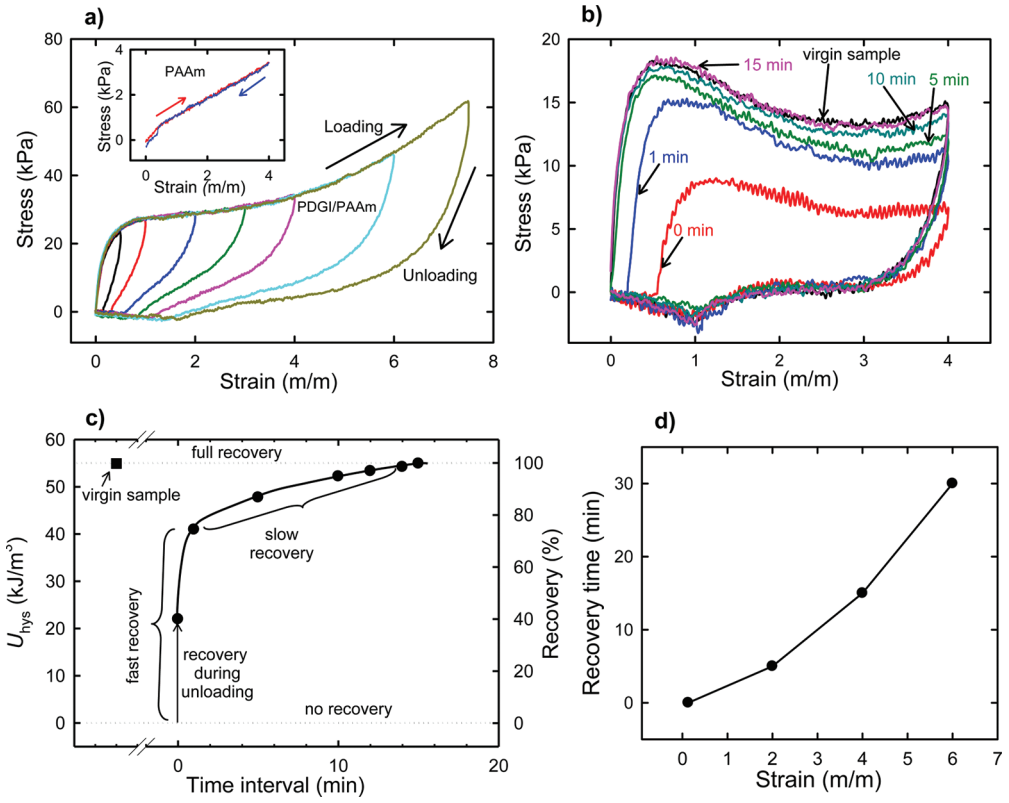

Figure 4. (a) Tensile loading−unloading curves of the PDGI/PAAm gel containing 0.13 M DGI exhibit as hysteresis. The hysteresis cycles are repeated with the same sample at increasing levels of maximum strain. All the loading curves are followed to their previous loading curve up to the maximum strain achieved in the previous one. There is no hysteresis for the pure PAAm gel which is also shown in the inset figure. (b) The first hysteresis cycle of the virgin PDGI/PAAm gel sample (0.1 M DGI) (black line) is repeated after different time interval such as 0 min (red), 1 min (blue), 5 min (green), 10 min (cyan), and 15 min (pink) using the same sample. At a time interval of 15 min, the hysteresis cycle (pink) is fully overlapped to the first cycle (black) indicating the full recovery of mechanical strength and dimensions of the gel. (c) The dissipated energy (area of hysteresis loop: U_{hys}) of different cycles performed with different time intervals and the recovery (%) is plotted against time interval to observe the time dependent self-recovery. For a strain of 4, 75% of the hysteresis area is recovered within 1 min and the rest need about 14 min. (d) Strain dependencies of full recovery time. The larger the strain achieved during loading required, the longer the time to recover completely.

loading−unloading experiments on the gel upon tension to a predefined tensile strain (Figure 4a). As expected for a conventional chemically cross-linked gel that is purely elastic, no hysteresis loop is appeared in the single PAAm gel (Figure 4a, inset). On the contrary, the loading−unloading curves of the bilayer incorporated gel deviated from one another during the same experiment, exhibiting a form of energy dissipation due to the structure change of the bilayer aggregates of PDGI. Since the hysteresis is observed even before the yielding point, the energy dissipation mechanism before and after the yielding are different, corresponding to different structure change. We assume that before yielding, the associated hydrophobic side groups of PDGI experience the plastic deformation under tensile stretching. Above the yielding strain, the polymer backbone of the PDGI that was in random coil conformation starts to be extensively elongated, so that the associated hydrophobic side groups are forced to dissociate. The latter process absorbs a large amount of energy for hydration, and increases the resistance against crack propagation. We investigated whether the hysteresis loops relate to a permanent damage due the tensile loading. The consecutive hysteresis cycles with the same sample at gradual increasing levels of maximum strain are shown in Figure 4a. All the cycles follow the same loading curves and different unloading curves, implying that the stiffness of the gel returns to its initial state after each deformation cycle, which is a clear indication of self-recovery of the initial stiffness of the gel upon successive loading with a rest time. This behavior shows a complete absence of Mullins effect in contrast with observations for the reported double network (DN) gels.[23] Significant hysteresis has been noted in the first loading cycle of DN gel, but no recovery was observed due to the permanent damage of chemical bonds in the brittle polyelectrolyte (PAMPS: 2-acrylamido-2-methylpropanesulfonic acid) network structure.[23,24] So, the rigid PDGI bilayers in the PDGI/PAAm gel serve as the reversible sacrificial bonds, whereas the brittle PAMPS network in the DN gel serves as irreversible sacrificial bond.

It is worth noting that a recovery time was required between two successive cycles to achieve the original dimensions and stiffness of the gel sample. To quantitatively characterize the time-dependent self-recovery, we performed multiple repeat of cycles at fixed maximum strain on the same sample with different time interval between two successive cycles (Figure 4b). The first loading−unloading cycle of the virgin sample exhibits hysteresis. The immediate second loading−unloading cycle of the same sample with a time interval of 0 min shows partial recovery of the hysteresis loop. The hysteresis loops of subsequent cycles increase with the increase in time interval, and finally at an interval of 15 min hysteresis is completely reproduced to that of virgin sample or first cycle, indicating the complete recovery of

dx.doi.org/10.1021/ma201653t |*Macromolecules* 2011, 44, 8916–8924

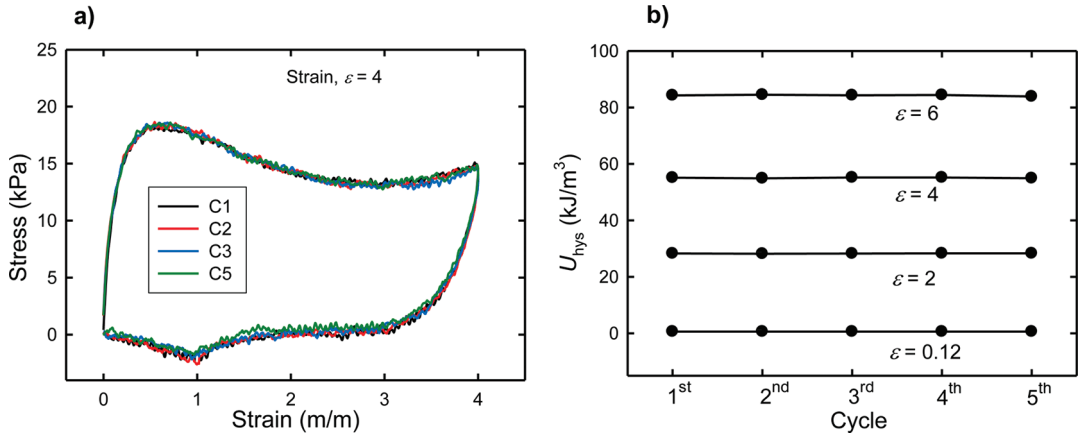

Figure 5. (a) Multiple repeat of loading−unloading hysteresis cycles of PDGI/PAAm gel (0.10 M DGI) at a maximum strain (ε) of 4. The first cycles (C1) of the virgin sample is fully overlapped to all the next repeated cycles (C2, C3, C5) of the same sample while a waiting time of 15 min is maintained before performing every repeated cycle. This indicates the multiple self-recovery or persistent fatigue resistance of the gel on successive loading with an interval or rest of 15 min. (b) Area of the hysteresis loop in terms of dissipated energy (U_{hys}) is found to be identical from 1st to 5th cycle when the multiple repeat of loading−unloading cycles are performed at different maximum applied strains demonstrating the fatigue resistance of the gel depend on both the applied strain and time interval between two successive loading.

the gel strength and dimensions within 15 min. The dissipated energy or area of the hysteresis loop (U_{hys}) for every cycle against time interval is shown in Figure 4c. At an interval of 0 min some extent of recovery can be noticed. Actually, this quick recovery occurred during the experimental unloading time (~15 s). Most of the hysteresis is recovered within 1 min, and then the slow recovery process takes relatively longer time (~15 min). This indicates two types of recovery processes of the structure. Both the quick and slow recovery of the strain is owing to the polymeric nature of PDGI and PAAm, driven by elastic and entropic restoring forces of PDGI backbone as well as PAAm network and the slow recovery of the strain is driven by the entropy. The recovery of the stress is attributed to the reassociation (fast) reorganization (slow) of the hydrophobic PDGI side groups driven by the high interfacial tension between PDGI hydrophobic chain and water. The quick recovery of the gel can be simply observed in Movie-2. The full recovery time further depends on the maximum strain applied during loading which is found to increase with the increase of strain (Figure 4d). At low tensile deformation (strain ~0.12) below the yielding, the bilayers are not destroyed and only few seconds is required to recover completely due to the interfacial tension between DGI hydrophobic chains. In contrast, at large deformation (strain >1) above the yielding, the bilayer is destroyed and the destruction become larger with the increase in strain, and consequently longer time (several minutes) is required to recover completely. Heating the material up to the temperature above 50°C induced the full recovery of dimensions and hysteresis in a few seconds to a similar level that achievable by slow recovery in several minutes at 25 °C.

Fatigue Resistance. We further checked whether the hysteresis loop is repeatable over a series of loading−unloading cycles, which is an indication of "fatigue resistance" of such materials. We performed multiple repeat of cycles at different maximum strain on the same sample with an interval of corresponding complete recovery time between two successive cycles. Figure 5a demonstrates the multiple repeat of cycles for an applied maximum strain of 4. All the subsequent hysteresis cycles (C2−C5) are reproducible to the first cycle of the virgin sample (C1). The dissipated energy or hysteresis area for all the cycles are also identical, as shown in Figure 5b (strain = 4). This is a clear indication of multiple self-recovery or fatigue resistance of the gel on several numbers of successive loading while the gel is deformed frequently with a time interval to a fixed strain. The hysteresis cycles are reproducible distinctly for different maximum strain (0.12, 2, and 6) (Figure S2), and the areas of the hysteresis cycles are also identical for every cycle at corresponding strain (Figure 5b). The repeated cycles for all strains can be reproducible even by using only one gel sample for all self-recovery measurements. So, the gel possesses superb ability to self-recover for several tens of successive loading.

Crack Resistance by Forming Huge Blunting. For a tough gel it is difficult to propagate a steady crack through the sample from a pre-existing crack. The PDGI/PAAm gel, especially, the lipid-like nature of the bilayers seems to be crucial for dramatically reducing the maximum stress at the crack tip, as shown by the pure shear fracture test in Figure 6 and Movie-2. When the gel having an initial crack/notch (Figure 6a) is elongated perpendicular to the crack direction, a huge blunting with an extraordinary pestle and/or trumpet shape occurs at the crack tip. As a result, there is no stress concentration at all in front of the crack tip, as revealed by the homogeneous blue shift of the gel color over the blunting and whole stretching area (Figure 6b−d). After releasing the stress, the gel recovered quickly to a small residual strain state (Figure 6e) and then recovered gradually back to the original dimension and color after several minutes, showing a very small crack propagation distance of about 1 mm (Figure 6f).

In contrast, in the case of the single PAAm gel, the crack easily propagates even at a small strain (Figure 6g and Movie-3). We assume that besides the yielding effect or molecular dissociation of the PDGI bilayers, the mobile or lipid-like nature of the bilayer is crucial to form the extraordinary blunting at the crack tip. The recovery of the bilayer structure driven mainly by elastic restoring force of the PDGI backbone, however, reveals the solid-like nature of bilayers. The delicate balance between the liquid-like and solid-like natures of the PDGI chains during stressing and releasing make it extraordinarily tough and self-recoverable.

The PDGI/PAAm hydrogel dissipates large amount of energy at fracture (the work of extension, $W_{ext} \sim 5 \times 10^6$ J m^{-3},

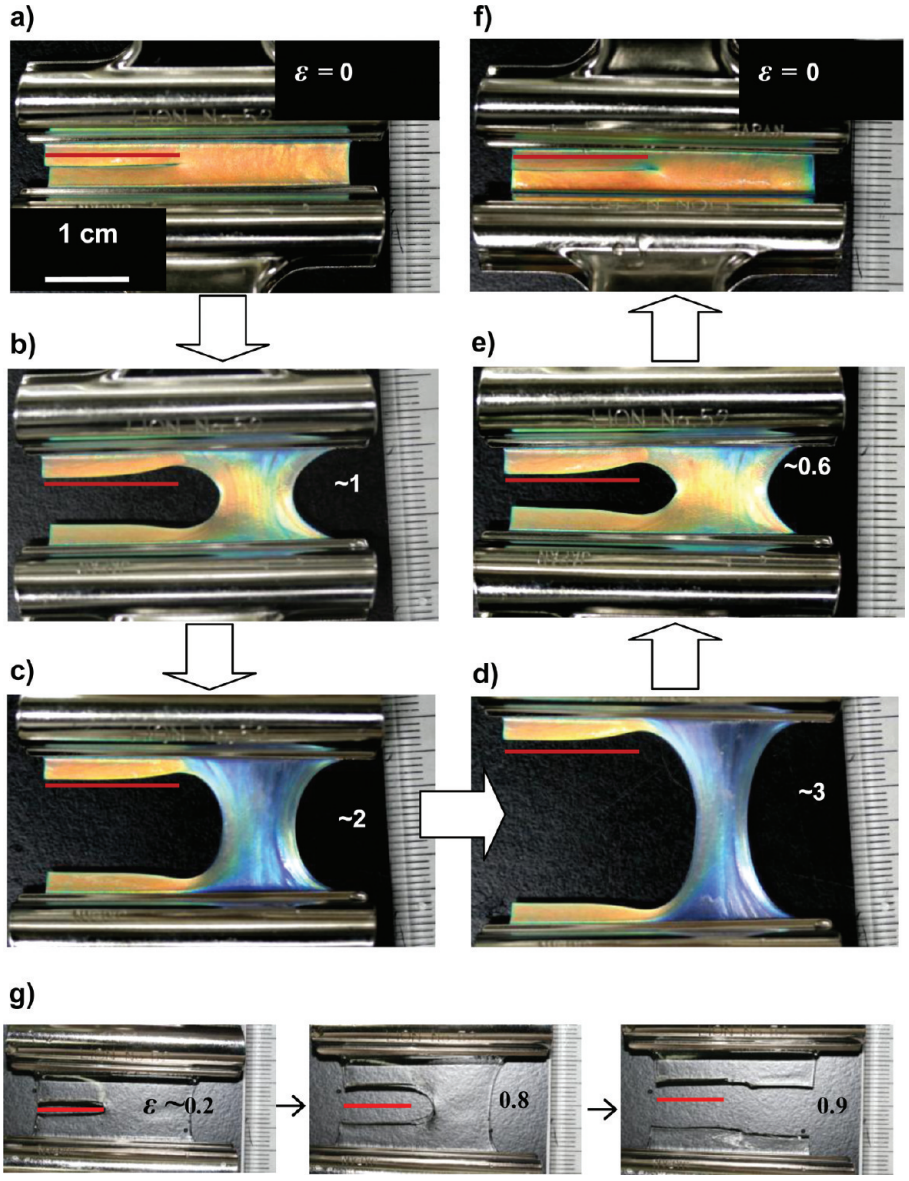

Figure 6. Crack resistance due to huge blunting during pure shear fracture test. The PDGI/PAAm gel (0.10 M DGI) was cut to have an initial sharp notch/crack along the longitudinal direction (a). The gel is stressed perpendicular to the crack direction up to a strain (ε) of about 3 or even more. A huge blunting occurs in front of the crack tip and it completely suppresses the stress concentration, simply as shown by the homogeneous structural color change of the gel over the blunting as well as whole stretching area (b, c, d). After release of stress, the gel quickly returns back to a small residual strain state (e) and finally recovers to its original dimensions and color after several minutes (f). This phenomenon is reversible and can be repeated for many times. (g) For single PAAm gel, crack propagates easily at small deformation (strain, $\varepsilon < 1$) due to stress concentration at the crack tip in contrast to the PDGI/PAAm gel. The red line in every image shows the initial crack distance.

Figure 2c), which is in the same order of tough DN gel.[13] The exceptional increase in mechanical strength and toughness of the bilayer incorporated hydrogel is attributed to the rigid but lipid-like nature of the bilayers, where the reversible and noncovalent hydrophobic association of PDGI serves as a sacrificial bond. This is superior to the tough DN gel that showed permanent damage, where the irreversible covalent bonds of brittle polyelectrolyte networks served as the sacrificial bonds.

■ CONCLUSIONS

In conclusion, single-domain lamellar bilayers not only diffracted visible light to exhibit magnificent structure color but also dramatically enhanced the mechanical strength and toughness of the hydrogel providing large hysteresis as an energy dissipation mechanism. This hydrogel with well-ordered stratified structure is in contrast to the most conventional hydrogels with amorphous structure which have negligible hysteresis and thus poor toughness. Lipid-like mobile nature of bilayers and their reversible molecular dissociation serve as a reversible sacrificial bond providing self-recovery and persistent fatigue resistance. Further, this lipid-like bilayer structure innovated a novel toughening phenomenon, crack blunting, into the soft hydrogel. This kind of toughening mechanism, therefore, is specific for the soft materials such as biological soft tissue in which both of the two components are from soft gel-like materials and does not occur

in the hard materials such as nacre in which one of the components is from hard solid. The excellent mechanical performances and unique toughening phenomena of the hydrogel could explore insight into the toughening mechanism of biological soft tissues with laminated structure. Moreover, this soft hydrogel delegates a strong bridge between the iridescence and the toughening mechanism of the biological body that possesses tough skin layer and exhibits color.

■ ASSOCIATED CONTENT

Supporting Information. Tensile stress−strain behaviors of the PDGI/PAAm gel with different DGI concentrations and multiple repeat of hysteresis cycles at strain of 0.12, 2, and 6. This material is available free of charge via the Internet at http://pubs.acs.org.

■ AUTHOR INFORMATION

Corresponding Author
*Tel: +81-11-706-2774. E-mail: gong@sci.hokudai.ac.jp.

■ ACKNOWLEDGMENT

This study was supported by a Grant-in-Aid for Specially Promoted Research (No. 18002002) from the Ministry of Education, Science, Sports and Culture of Japan. The synchrotron radiation experiments were performed at BL40B2 in SPring-8 with the approval of the Japan Synchrotron Radiation Research Institute (JASRI) (Proposal No. 2009A1349). The authors thank H. Furukawa and H. Masunaga for the help of experiments.

■ REFERENCES

(1) Currey, J. D. *Proc. R. Soc. London, B* **1977**, *196*, 443–463.
(2) Jackson, A. P.; Vincent, J. F. V.; Turner, R. M. *Proc. R. Soc. London, B* **1988**, *234*, 415–440.
(3) Okumura, K.; de-Gennes, P. G. *Eur. Phys. J. E* **2001**, *4*, 121–127.
(4) Kamat, S.; Su, X.; Ballarini, R.; Heuer, A. H. *Nature* **2000**, *405*, 1036–1040.
(5) Rao, M. P.; Sanchez-Herencia, A. J.; Beltz, G. E.; McMeeking, R. M.; Lange, F. F. *Science* **1999**, *286*, 102–105.
(6) Fung, Y. *Biomechanics: Mechanical Properties of Living Tissue*, 2nd ed.; Springer-Verlag, Inc.: New York, 1981.
(7) Langer, R.; Tirrell, D. A. *Nature* **2004**, *428*, 487–492.
(8) Peppas, N. A. *Hydrogels in Medicine and Pharmacy*; CRC Press: Boca Raton, FL, 1987.
(9) Okumura, Y.; Ito, K. *Adv. Mater.* **2001**, *13*, 485–487.
(10) Sakai, T.; Matsunaga, T.; Yamamoto, Y.; Ito, C.; Yoshida, R.; Suzuki, S.; Sasaki, N.; Shibayama, M.; Chung, U. *Macromolecules* **2008**, *41*, 5379–5384.
(11) Haraguchi, K.; Takeshita, T. *Adv. Mater.* **2002**, *14*, 1120–1124.
(12) Gong, J. P.; Katsuyama, Y.; Kurokawa, T.; Osada, Y. *Adv. Mater.* **2003**, *15*, 1155–1158.
(13) Gong, J. P. *Soft Matter* **2010**, *6*, 2583–2590.
(14) Lin, W. C.; Fan, W.; Marcellan, A.; Hourdet, D.; Creton, C. *Macromolecules* **2010**, *43*, 2554–2563.
(15) Henderson, K. J.; Zhou, T. C.; Otim, K. J.; Shull, K. R. *Macromolecules* **2010**, *43*, 6193–6201.
(16) Tsujii, K.; Hayakawa, M.; Onda, T.; Tanaka, T. *Macromolecules* **1997**, *30*, 7397–7402.
(17) Haque, M. A.; Kamita, G.; Kurokawa, T.; Tsujii, K.; Gong, J. P. *Adv. Mater.* **2010**, *22*, 5110–5114.
(18) Ozawa, J.; Matsuo, G.; Kamo, N.; Tsujii, K. *Macromolecules* **2006**, *39*, 7998–8002.
(19) Tominaga, T.; Tirumala, V. R.; Lee, S.; Lin, E. K.; Gong, J. P.; Wu, W. L. *J. Phys. Chem. B* **2008**, *112*, 3903–3909.
(20) Hawkes, J. W. *Cell Tiss. Res.* **1974**, *149*, 159–172.
(21) Liu, Y.; Shigley, J.; Hurwit, K. *Opt. Express* **1999**, *4*, 177–182.
(22) Ito, K. *Polym. J.* **2007**, *39*, 489–499.
(23) Weber, R. E.; Creton, C.; Brown, H. R.; Gong, J. P. *Macromolecules* **2007**, *40*, 2919–2927.
(24) Tanaka, Y. *Europhys. Lett.* **2007**, *78*, 56005; 1−5.